

Land Surface Roughness Effects on Lake Effect Precipitation

Brent M. Lofgren*

NOAA/Great Lakes Environmental Research Laboratory
2205 Commonwealth Blvd.
Ann Arbor, Michigan 48105

ABSTRACT. *The land use of the Great Lakes region has changed significantly during historical times, and continues to change. As a preliminary step in investigating the overall effect that this might have on climate, attention is focused here on one forcing factor and one effect—land surface roughness length and lake effect precipitation, respectively—that are anticipated to be particularly sensitive pieces of the land use-climate interaction. On both a monthly basis and in an individual case of lake effect precipitation, a reduction of land surface roughness reduces the total amount of lake effect precipitation. It also reduces the degree to which the precipitation is focused on the area closest to the lakeshore. The largest reductions occur immediately adjacent to the lakeshore in an area smaller than the overall lake effect zone. In the individual lake effect event that is investigated here, precipitation increases in some places farther inland when surface roughness is reduced. Because this increase in precipitation farther inland appears to be associated with significant topography, this result is most valid for lake effect zones where there is a high topographic relief, such as near southeastern Lake Erie (the main focus of this study), and to the south and east of Lake Ontario. This displacement in location of precipitation is particularly crucial where the boundary of the drainage basin is near the shoreline, and can indicate a flux of moisture out of the Great Lakes drainage basin and into another basin.*

INDEX WORDS: *Lake effect precipitation, land use, atmospheric modeling,*

INTRODUCTION

Lake effect precipitation (both snow and rain) plays an important role in the weather and hydrology of many regions near the shores of the Laurentian Great Lakes. The heaviest lake effect precipitation generally falls during the fall and early winter on the eastern or southeastern shore of each lake, where the prevailing winds are onshore. Niziol *et al.* (1995) summarize some of the key conditions needed for the production of lake effect and some sub-types of lake effect. This paper will be concerned with what Niziol *et al.* (1995) refer to as Type I and Type II lake effect events. Type I has wind blowing along the long axis of a lake. It tends to develop a single strong band of precipitation parallel to the wind, dropping precipitation on the lake and also at the shoreline. Type II lake effect has wind along the short axis of a lake and has several more diffuse bands of precipitation. Again, these can deposit precipitation both over the lake and on the shore.

The lake effect events happen during cold air out-

breaks, generally in the fall to early winter, when the lakes are considerably warmer than the air overlying them. This helps to fulfill one of the major conditions for lake effect precipitation—the lower atmosphere must be unstable. According to Holroyd (1971), the required threshold is that lake surface temperatures must be at least 13°C warmer than the air at 850 mb. This quantity corresponds to the dry adiabatic lapse rate, making the lower part of the air column statically unstable, and enabling the heat from the lake to erode and eliminate any inversion that may exist below the 850 mb level, as often occurs over land in a subsiding cold air mass. This erosion of the inversion creates a thick layer with a near-neutral buoyancy profile.

Hjelmfelt (1990) carried out numerical simulations of scenarios of lake effect precipitation, and investigated the impact of a variety of factors on the amount of precipitation that falls in a given event. Parameters for which sensitivity was tested include lake-land temperature difference, static stability of the air, ambient wind speed, wind direction, humidity over the land, friction, and Coriolis effect. In general, lake effect precipitation occurred when

*Corresponding author. Brent.Lofgren@noaa.gov

there was sufficient lake-land temperature difference and low enough static stability. In these simulations, there was sometimes seen to be an optimum wind speed of intermediate value. The wind direction had an important effect, mainly attributed to its influence on fetch over the lake. The influx of moisture from the land near the lake effect zone, as affected by the relative humidity of the air over land, was shown to significantly affect the quantity of lake effect precipitation. Of the various combinations of surface roughness on lake and land tested by Hjelmfelt (1990), the highest amount of precipitation occurred when both the land and the lake had high surface roughness. Low Coriolis effect, corresponding to latitudes closer to the equator, results in greater amounts of lake effect precipitation. Hjelmfelt (1992) investigated the effect of including vs. excluding orography, and found that orography, i.e., the forcing of air upward as it reaches shore, enhances lake effect precipitation.

Laird and Kristovich (2004) further investigated the influence of wind fetch over the lake, comparing the numerical modeling results of Laird *et al.* (2003a, b) to observations. They found that the quantity U/L (wind speed divided by length scale) is important in determining the quantity of precipitation in near-shore snow-band types (Types I and II of Niziol *et al.* 1995). The value of L (the denominator of U/L) is highly dependent on the wind direction, i.e., whether the wind is blowing along the long axis or short axis of the lake. They found U/L to be less important in the midlake and mesoscale vortex type lake effect events (Types IV and V of Niziol *et al.* 1995). U/L has units of inverse seconds, and is a measure of the (inverse) amount of time that air parcels spend over the lake.

Besides wind (for Types I and II lake effect) and unstable air, forced upward motion is an important ingredient in lake effect precipitation. Three major mechanisms can lead to upward motion: 1. Thermally-forced motion. This is most important in Type IV and Type V lake effect precipitation, as defined by Niziol *et al.* (1995). Passarelli and Braham (1981) highlight the importance of thermally forced land breezes leading to low-level convergence over the lake, resulting in snow bands parallel to the shore. 2. Orographic uplift, as reported by Hjelmfelt (1992). 3. Motion forced by frictional convergence at low levels near a shoreline.

The thermal influence of the Laurentian Great Lakes as a group on the atmosphere in a cold-air outbreak environment can result in a surface low pressure system at the meso- α scale, i.e., on the

order of 1,000 km, and thus incorporating in a significant way both geostrophic and ageostrophic motion (Sousounis and Fritsch 1994). Further evidence of this is present in the charts of 850-mb height from aggregates of lake-effect events presented by Liu and Moore (2004). This lake-aggregate vortex and the accompanying thermal effects on the atmosphere can alter the environment at the spatial scale corresponding to the group of Great Lakes and thus influence the formation and intensity of snowfall on the scale of individual lakes (Sousounis and Mann 2000).

Motivated by historical changes in land use in the Great Lakes region (Cole *et al.* 1998), this paper will investigate some of the possible effects of land use change on the regional climate system. It focuses on the model simulation of one of the primary anticipated interactions—that between land surface roughness and lake effect precipitation. The next section describes the model that is used here. The section after that describes the experimental design using that model. The results section presents changes in precipitation during December 1993 resulting from changes in land surface roughness and then concentrates on a shorter time period on 11 December 1993, diagnosing the circulation and resulting precipitation. Finally, some concluding remarks are included in the last section.

MODEL

This study makes use of the Coupled Hydrosphere-Atmosphere Research Model version 2 (CHARM 2). CHARM 2 uses as its atmospheric component the Regional Atmospheric Modeling System version 4.4 (RAMS 4.4; Pielke *et al.* 1992, Cotton *et al.* 2003), and couples this with an array of one-dimensional thermodynamic water column models, based on the formulation of Hostetler and Bartlein (1990). Conceptually, CHARM 2 is similar to the original version of CHARM (Lofgren 2004), but several changes have been implemented, as highlighted below.

A standard feature of RAMS 4.4 that is used in CHARM 2 is the more sophisticated land surface component known as LEAF-2 (Walko *et al.* 2000). This component calculates the latent and sensible heat and radiative fluxes exchanged among the atmosphere, vegetation canopy, and soil. It uses this information to prognostically determine the temperature of the canopy and the soil profile. LEAF-2 also includes a prognostic model of the snowpack.

The parameterization of lake temperature that

was used in the previous version of CHARM, which treated each lake as having a water column that was horizontally uniform, has been replaced by an array of 1-dimensional water columns that prognostically determine water temperature according to the formulation of Hostetler and Bartlein (1990). This formulation takes into account wind stress at the surface and static stability of the water column in order to determine a coefficient of vertical diffusion.

When the water surface reaches 0°C, any additional heat loss is accounted for as ice formation to determine a mean ice thickness. At mean ice thickness less than 10 cm, the fractional coverage of ice is taken as the mean thickness divided by 10 cm; at mean ice thickness greater than 10 cm, the fractional coverage is considered to be 1. As ice forms, heat budgets are calculated separately for ice and liquid water, and the surface-atmosphere flux is taken as an average of these, weighted according to the area of each. The albedo of lake ice is taken as a linear function of temperature between 0.45 at 0°C and 0.6 at -10°C, and a constant value of 0.6 at temperatures less than -10°C.

EXPERIMENTAL DESIGN

In order to determine the sensitivity of CHARM 2 and its simulated lake effect precipitation to large-scale changes in land surface roughness throughout the Great Lakes region, we compare the results of a standard roughness case, in which the default values are assigned for all land cover parameters, and the grass roughness case in which the surface roughness length is changed over all land areas so that it does not exceed 0.1 m, a value corresponding to tall grass. Much of the northern part of the domain is designated as evergreen needleleaf trees, with a surface roughness length of 1.0 m, while some of the more southern part is broadleaf deciduous trees, with a surface roughness length of 0.8 m. Most other areas are cropland or tall grass, with surface roughness length of 0.1 m.

Land cover is handled in a tile approach, in which each grid cell is designated as having fractional portions in various land cover types. The fluxes of quantities that are exchanged between the surface and the atmosphere—momentum, sensible heat, and water vapor/latent heat—are calculated separately for each tile, then area weighted and aggregated to get a net flux to the atmosphere. The mean surface roughness length used in the standard roughness case is mapped in Figure 1 for the por-



FIG. 1. Mean surface roughness length (meters) used in the standard roughness case. Fractional parts of each grid cell can have different land cover types and hence different surface roughness lengths. Contours are shown for values from 0.1 to 0.7 m, with dashed contours for values below 0.5 m. No land areas have surface roughness lengths greater than 0.8 m. Grid cells that are completely covered by water are assigned a default roughness length of 2.0 m that is used for purposes of this figure, but see the text for the treatment of roughness length over water.

tion of the domain that is the area of concentration later in this paper. Areas east and southeast of Lake Erie have surface roughness lengths near the deciduous broadleaf value of 0.8 m, while areas near the western part of Lake Erie and to its north have lower values. For grid cells that are entirely covered by water, a default value of 2.0 m is assigned for purposes of mapping in Figure 1, but the roughness over water is calculated using the Charnock relation, which gives water surface roughness as a function of frictional wind speed.

The CHARM 2 model was configured on a domain centered at 45° N, 84°W. The horizontal grid spacing is 40 km, with 53 grid spaces in the east-west direction and 43 grid spaces in the north-south direction. While not resolving the individual elements of lake-effect precipitation complexes, this model will show some of the gross features of effects on areally averaged dynamics, particularly vertical velocity, and derive a resultant approximation of precipitation at the scale resolved by the model.

In the vertical, the lowest model layer is centered at a sigma-z value of 47.7 m and is 100 m thick in sigma-z coordinates. There are 23 vertical layers, with the model top at 21,043 m above mean sea

level. (The sigma-z coordinate system is defined with height scaled by the distance between the local surface and the model top and offset by the surface elevation, so that sigma-z = 0 m is at the surface, sigma-z = 21,043 m is at a constant height above sea level, low values of sigma-z approximate the height above the surface, and values near the maximum approximate the height above mean sea level. See Pielke *et al.* 1992.)

Both the standard roughness and grass roughness model cases were initialized with data from the NCEP/NCAR Reanalysis dataset (Kalnay *et al.* 1996) at 00Z 1 January 1993. They were run for a full year with nudging toward the NCEP/NCAR Reanalysis data in the outermost 5 grid points of the domain. Soil moisture was initialized at half its saturation value throughout the domain, and lake temperatures were initialized at 3.98°C throughout the column.

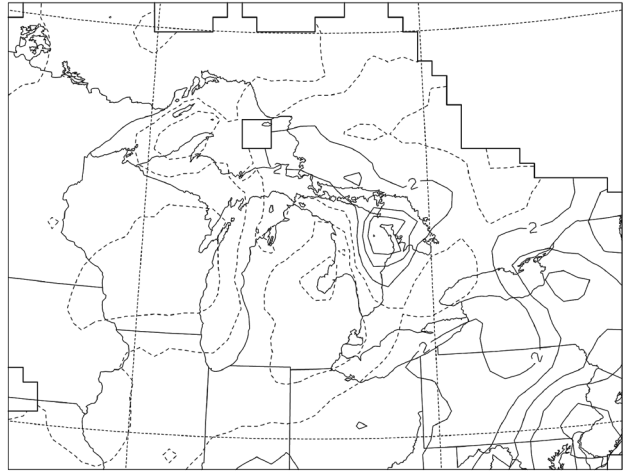
RESULTS

Monthly Precipitation—December 1993

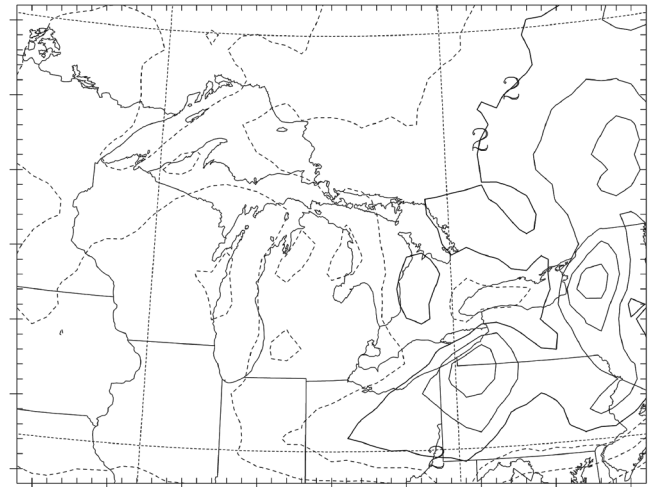
The total precipitation distribution in the Laurentian Great Lakes region during December 1993 shows concentrations in the lake effect zones (Fig. 2a, b). The observations in Figure 2a are derived by inverse-distance weighted interpolation from the fully quality-controlled Summary of the Day data at cooperative observing stations in the region, distributed by the National Climate Data Center for the U.S. and Environment Canada for Canadian stations. The lake effect zones are located generally near the eastern side of each of the lakes. The strongest centers of lake effect precipitation in the standard roughness simulation (Fig. 2b) are near the southeastern margin of Lake Erie and just to the east of Lake Ontario. On the other hand, the obser-

FIG. 2. Monthly mean precipitation rate for December 1993 according to (a) observations and (b) simulation by the standard roughness case of CHARM 2. The contour interval is 0.5 mm/day; solid contours indicate values of 2 mm/day and above, and dashed contours indicate lesser values. (c) The grass roughness case minus the standard roughness case. The contour interval is 0.1 mm/day with an additional contour of -0.05 mm/day added to emphasize the negative impact on precipitation east of Lake Michigan; solid contours indicate values of 0 or higher, and dashed contours are negative values.

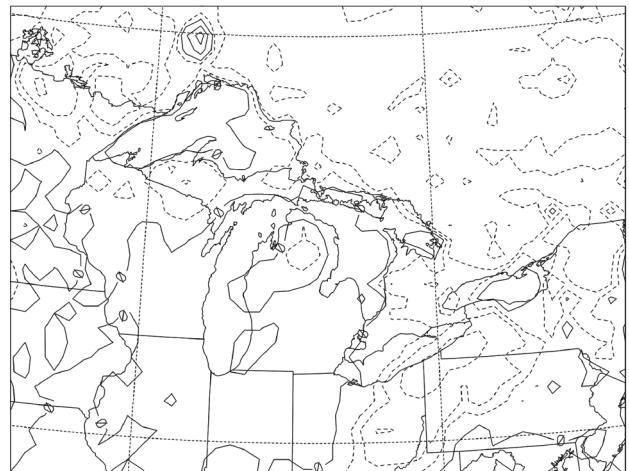
a. December 1993 observed precipitation



b. December 1993 precipitation—model standard roughness



c. December 1993 precipitation—grass minus standard roughness



vations (Fig. 2a) show the greatest concentration over the Bruce Peninsula in eastern Lake Huron, farther north than the secondary maximum of precipitation near southeastern Lake Huron shown in Figure 2b. Areas of enhanced precipitation over this month-long period are also present in both observation and simulation, at varying intensity, near the east sides of Lake Michigan and Lake Superior. One factor at work in the lake effect zones of Lakes Erie and Ontario is the enhancing effect of topography on lake effect precipitation (Hjelmfelt 1992); CHARM 2 may be exaggerating this influence. The lake effect zones corresponding to the other Great Lakes have less topographic relief, although it can still play some role. The locations of these simulated precipitation centers agree well with observations. Additionally, superimposed on this pattern is an east-west gradient in precipitation on the scale of the entire domain, which seems to be faithfully reproduced by CHARM 2, with the exception of the southern edge of the domain, which manifests the effects of matching of lateral boundary conditions.

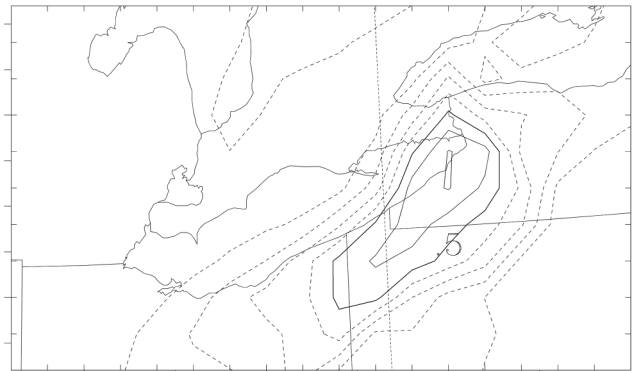
When surface roughness is reduced, the magnitude of the lake effect zones is reduced (Fig. 2c). In particular, the precipitation on the southeastern flank of Lake Erie is reduced (in the vicinity of 42°N , 80°W). The reduction in precipitation due to reduction in surface roughness shown in Figure 2c has a different shape from the maximum in precipitation shown in Figure 2b, with the latter being more round and extending farther inland and the former more oblong and concentrated along the shore of Lake Erie. This suggests that the mechanism for the overall precipitation rate is more spatially widespread than the mechanism by which precipitation is altered by a change in surface roughness.

Lake Effect Precipitation Event, 10–11 December, 1993

A particular event that had significant precipitation on the lee side of Lake Erie occurred on the night of 10–11 December, 1993 (local time). We analyze the time period 00Z to 06Z 11 December, when the greatest amount of precipitation fell on the southeastern shore of Lake Erie. While other events show more of a pattern of synoptic-scale precipitation enhanced and focused by the lake effect, this event has more of a pure lake-effect character, i.e., it has precipitation located exclusively in the lake effect zones.

In the standard roughness case, precipitation oc-

a. 6-hour precipitation standard roughness



b. 6-hour precipitation grass minus standard roughness

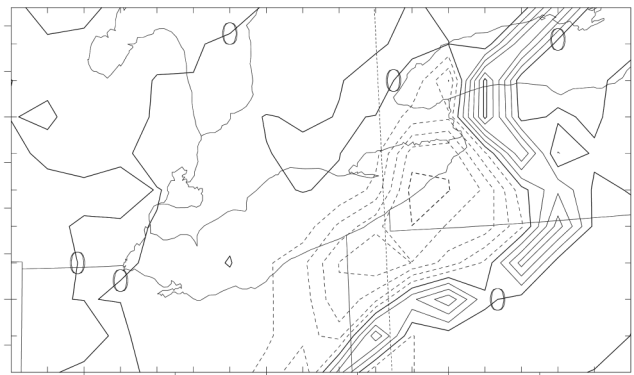


FIG. 3. Mean precipitation rate during the period from 00Z to 06 Z 11 December 1993 for a selected portion of the CHARM 2 domain. (a) The standard roughness case, with a contour interval of 0.1 mm/hour, values of 0.5 mm/hour shown by solid contours, and lesser values shown by dashed contours. (b) The grass roughness case minus the standard roughness case, with a contour interval of 0.05 mm/hour, negative values shown with dashed contours, and values of zero and above shown with solid contours.

curs along the southeastern shore of Lake Erie, with the greatest concentration near the eastern point of the lake (Fig. 3a). Most of the precipitation occurs within about 100 km of the shore. The placement of the main center of lake effect precipitation southeast of eastern Lake Erie during this time period is in qualitative agreement with observations. However, the daily aggregation of the cooperative observing network and the spatial contrast between the station observations and the grid-based simulation make direct comparison problematic. While the precipitation at this time is located mainly in the

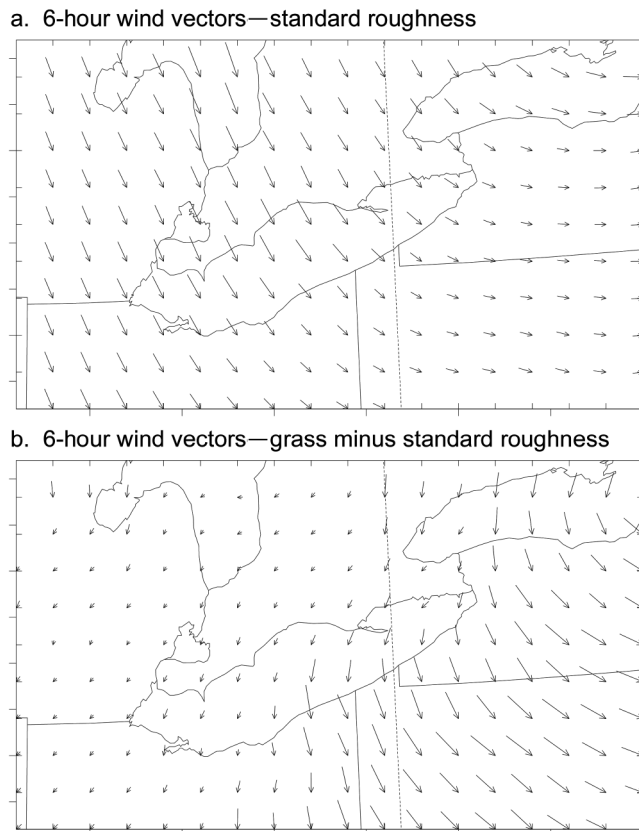


FIG. 4. Mean wind vectors during the period from 00Z to 06 Z 11 December 1993 at the lowest model level (approximately 48 m above ground level). (a) The standard roughness case. The distance between the tails of adjacent vectors is equivalent to 17 m/s. (b) The grass roughness case minus the standard roughness case. The distance between the tails of adjacent vectors is equivalent to 2 m/s.

vicinity of Lake Erie, local maxima can also be seen near Lake Huron at the top center of Figure 3a, and near Lake Ontario in the top right. As a result of reduced surface roughness, precipitation is both reduced and displaced (Fig. 3b). The location of maximum reduction in precipitation corresponds closely to the locations of maximum precipitation depicted in Figure 3a, and the reductions cover roughly the same area as the significant precipitation in Figure 3a. However, there are sharp features of increased precipitation in Figure 3b around the southern and eastern edges of the lake effect precipitation zone. Thus, although the overall amount of lake effect precipitation simulated for this event over the land near southeastern Lake Erie is re-

duced due to reduced surface roughness, it spreads to cover a larger area.

The surface winds blow from the northwest directly toward the southeastern shore of Lake Erie in the standard roughness case (Fig. 4a). Upon reaching the shore, these winds reduce in magnitude and curve toward the east, consistent with Ekman transport. This change in magnitude and direction of the wind vector occurs within about 100 km of the shore, in the region where the lake effect precipitation is occurring. The difference in surface wind vectors in the grass roughness case (Fig. 4b) shows an increase in the magnitude of wind in the southeastern portion of the illustrated area. The land in this area has higher surface roughness in the standard roughness case than do the areas farther west and north (Fig. 1). The increased wind occurs not only over the land downwind of Lakes Erie and On-

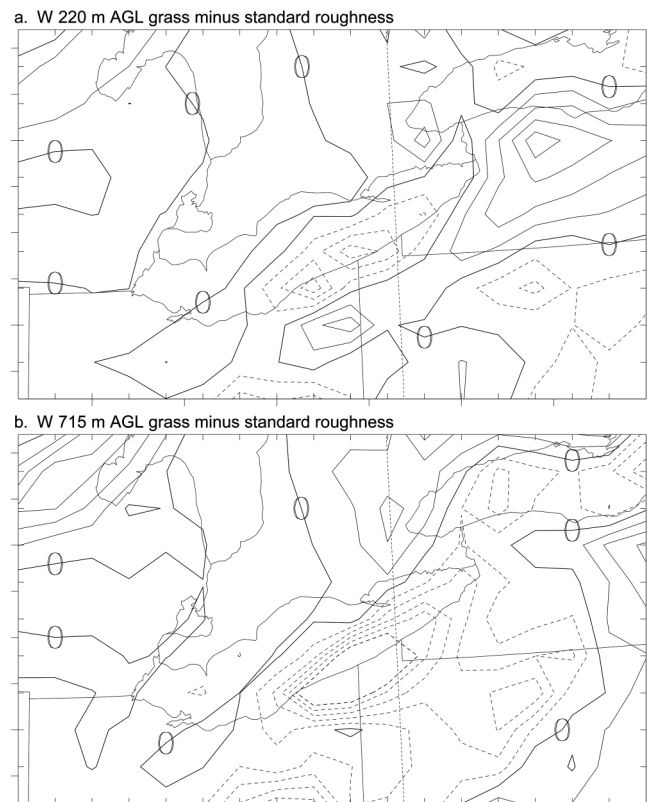


FIG. 5. Change in vertical velocity (cm/s), grass roughness case minus standard roughness case for (a) the second model level above the ground (approximately 220 m above the ground) and (b) the fifth model level above the ground (approximately 715 m above the ground). The contour interval is 0.2 cm/s, with dashed contours indicating negative values.

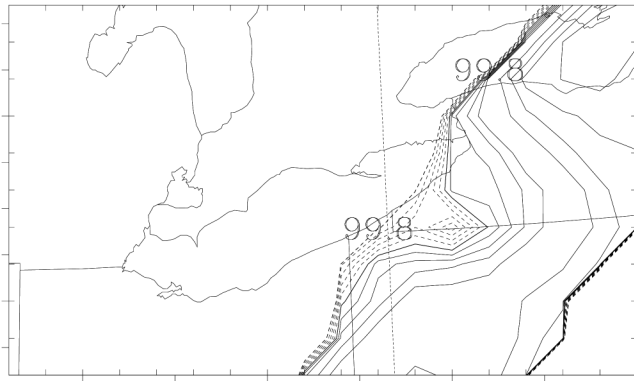


FIG. 6. *Relative humidity in the standard roughness case (percent) at approximately 45 m above the surface. Contours are shown only for values above 99.8 percent, with a contour interval of 0.02 percent. Values below 99.9 percent are shown with dashed contours.*

tario, but also over the lakes themselves. This effect over the lakes is due to a reduction in the local maximum in pressure just downwind of the lake (not shown), where air “piles up” after converging at the shoreline. Onshore, the increased wind speed is primarily due directly to reduced surface roughness. The southward component of the wind is particularly enhanced, because of the reduced Ekman transport toward the east.

The change in vertical velocity at low levels due to reduction in land surface roughness length (Fig. 5a, illustrated at the model’s second level above the surface, approximately 220 m above the ground) shows much correspondence with the changes in precipitation (Fig. 3b). It has a strong area of relative downward motion (i.e., a reduction in upward motion) in the region near the southeastern shore of Lake Erie. To the south and east of this are areas of relative upward motion. However, these regions have a broader extent than the band of increased precipitation in Figure 3b. At least part of the reason for this relative upward motion is upslope forcing from the ambient winds (Fig. 4a). At a higher level, approximately 715 m above the ground (Fig. 5b), these regions of relative upward velocity are eliminated, and all of the land to the south and east of Lake Erie has relative downward motion, with the highest magnitude still located along the shoreline. This indicates that any relative upward motion in the lake effect region as a result of reduced land surface exists only in a shallow layer.

The narrow band of increased precipitation in Figure 3b corresponds closely to the location of the

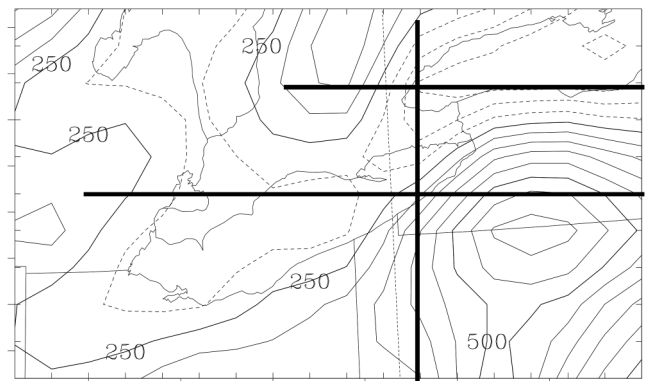
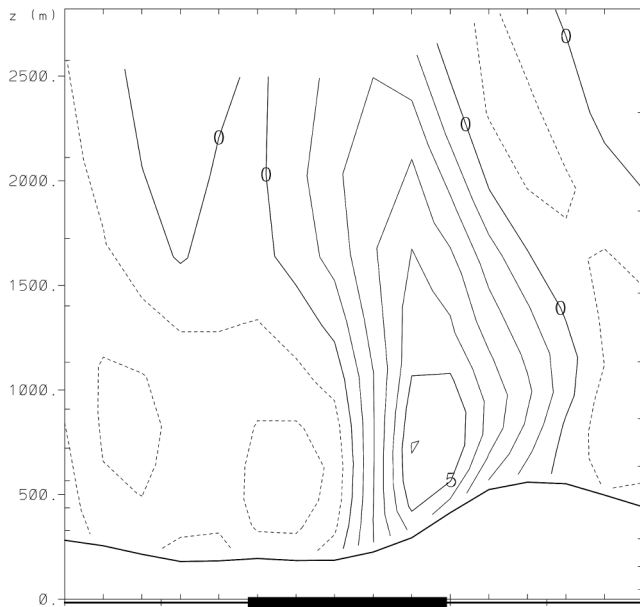


FIG. 7. *Topography in the region near Lake Erie, as used by CHARM 2. The contour interval is 50 m; values of 250 m above mean sea level and greater are shown by solid contours, and lesser values by dashed contours. The heavy lines indicate the locations of the vertical profiles in the following figures.*

highest relative humidity in the standard roughness case (Fig. 6). This location corresponds approximately to local maxima in topography (Fig. 7), or just to the east of those maxima, giving some indication that the highest values of relative humidity are caused by upslope winds adiabatically cooling the air until it approaches or reaches saturation. This reason is not adequate to explain the band of maximum humidity and increased precipitation that extends across Lake Ontario, however. Judging from the intense gradient in relative humidity to the northwest of this band and lesser gradient to the southeast, it seems to be associated with a frontal boundary, with colder air impinging on a region of higher moisture content. However, a discrete front is much less evident in plots of the wind (Fig. 4a), potential temperature (not shown), and water vapor mixing ratio (not shown). It should be noted, too, that high relative humidity and consequent large amounts of low-level cloudiness are known biases of CHARM 2 and its parent model, RAMS 4.4. Hence only very high values of relative humidity are contoured in Figure 6.

While some of the areas where precipitation is increased due to reduced surface roughness are associated with enhanced upslope winds, some are not. In particular, the region of reduced precipitation extends as far east as the location of maximum topographic height, while much of the enhanced precipitation occurs east of the maximum height.

a. W—standard roughness, profile 1



b. W—grass minus standard roughness, profile 1

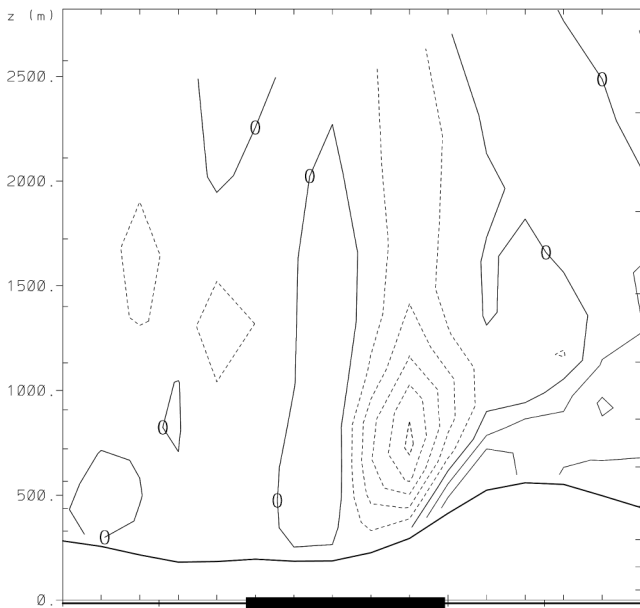


FIG. 8. Profiles of mean vertical velocity component during the period from 00Z to 06 Z 11 December 1993 along profile 1 shown in Figure 7. (a) The standard roughness case, with a contour interval of 1 cm/s. (b) The grass roughness case minus the standard roughness case, with a contour interval of 0.2 cm/s. In both panels, values of 0 and greater are shown by solid contours, and negative values by dashed contours. The location of Lake Erie is denoted by a dark bar at the bottom.

Wind velocity components are examined as profiles from single rows and columns of grid points shown in Figure 7. Starting with the east-west profile labeled as profile 1, the vertical velocity in the standard roughness case (Fig. 8a) has a tripole character. Near and just downwind of the shoreline, there is strong upward motion. This is forced by a combination of upslope flow and low-level convergence due to the contrast in surface roughness between the lake and land, and enhanced by thermal forcing from latent heat release as water condenses out of the atmosphere. This upward motion is much diminished at the 2,500 m level (all height references in this discussion are above mean sea level), indicating divergent horizontal winds through the range of roughly 800 to greater than 2,500 m. West of this region, over Lake Erie and also to its west, there is general subsidence and evidence of convergent flow in the 700 to 2,500 m range, and divergence below that. In the eastern part of this profile, there is downward motion corresponding to downslope winds, extending to heights greater than 2,500 m. These regions of downward motion comprise a compensation, or return, of the upward motion near the shoreline.

The magnitude of the upward motion near the shoreline is decreased as a result of reduced surface roughness (Fig. 8b), especially on the western side of its maximum from Figure 8a. Furthermore, this reduction in upward velocity is mainly restricted to levels below about 1,200 m, implying that this is the layer most strongly affected by the low-level convergence of wind due to surface roughness, while the higher levels may be more influenced by upslope wind forcing. In the eastern part of the profile, there is enhanced upward motion. On the western (upslope) side of the maximum topographic height, the increased upward velocity is restricted to quite near the surface, in agreement with the comparison of Figure 4a to Figure 4b, but it extends higher farther east.

A profile of eastward velocity in the standard roughness case (Fig. 9a) indicates that there is horizontal divergence near the shoreline at heights of about 800 m to greater than the 2,500 m level, albeit with magnitude diminishing with height. The region near the ground, to about 500 m, shows the opposite gradient in wind speed, that is, convergent wind. This single component of the horizontal wind has a qualitative consistency with the vertical velocity profile of Figure 8a.

The changes in eastward wind speed due to reduced surface roughness are shown in Figure 9b.

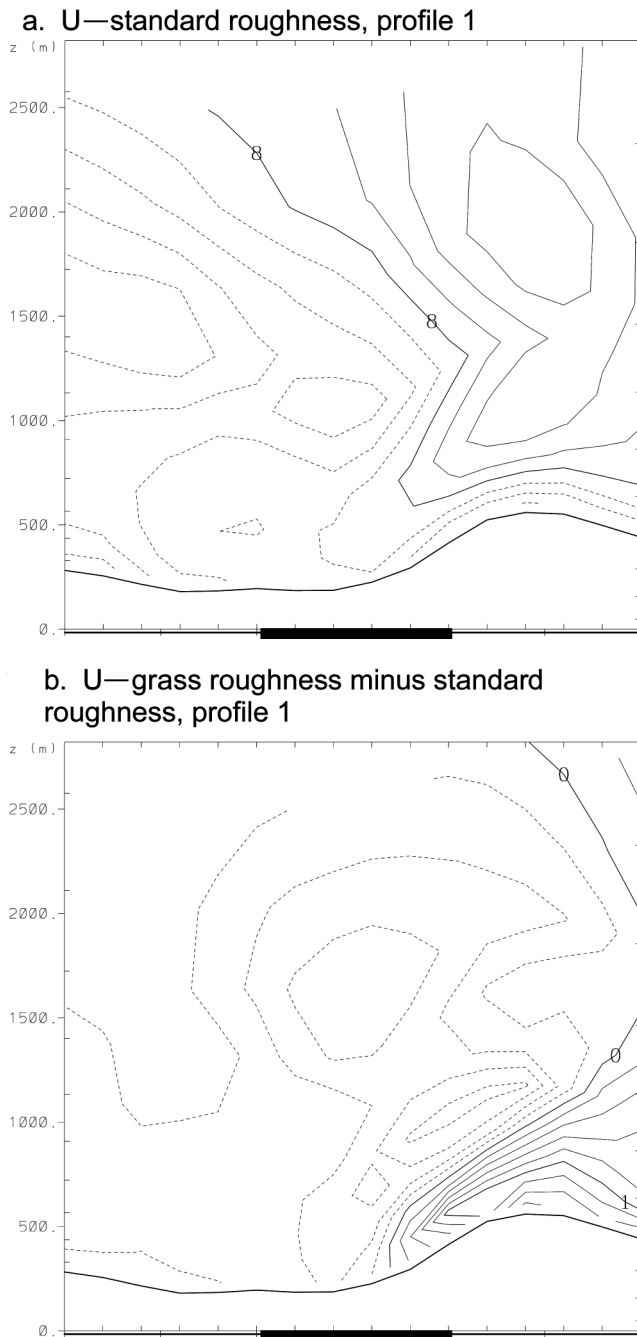


FIG. 9. As in Figure 8, but for the eastward component of wind, in model coordinates. In panel (a), the contour interval is 1 m/s, values of 8 m/s or greater are indicated by solid contours and lesser values by dashed contours. In panel (b), the contour interval is 0.2 m/s, values of 0 and greater are indicated by solid contours, and negative values by dashed contours. The location of Lake Erie is denoted by a dark bar at the bottom.

The slight reduction in the eastward component over the lake is associated with the clockwise rotation of the wind vectors evident in Figure 4b due to reduced Ekman forcing. But onshore to the east, a layer of higher wind speed develops near the surface due to the direct effect of the reduced surface roughness. Progressing farther eastward, the internal boundary layer associated with the land, and the associated layer of higher wind speeds, becomes deeper. Throughout the land area, there are increased wind speeds closer to the surface, and reduced wind speeds at higher levels, indicative of reduced turbulent transport of momentum toward the surface, as would be expected with the reduction in surface roughness. The slant in the isosurfaces of change in horizontal wind speed means that there is relative divergence in the winds. This relative divergence is concentrated near 600 m height at the shore, thus restricting the height of enhanced upward motion, but rises near 1,000 m east of the topographic maximum, allowing relative upward motion to penetrate to greater heights. Additionally, while the contours between about 800 m and 1,500 m slope upward at the eastern extreme of the profile, those below 800 m slope downward. The former indicates divergent flow at higher levels, reducing the enhanced upward motion to small values above 1,500 m, and as stated before is associated with a deepening internal boundary layer associated with the land. The latter indicates convergent flow sufficient to overpower enhanced downslope wind and produce relative upward motion and allowing precipitation in this region; its causes are less certain.

Along a north-south transect of Lake Erie, designated as profile 2 in Figure 7, a similar picture of vertical motion emerges. In the standard roughness case (Fig. 10a), there is a region of upward motion over the southern shore of the lake, with compensating downward flow over the lake and on its opposite side. Both of these occur to a height of 2,000 to 2,500 m. This is qualitatively similar to Figure 8a, but lacks evidence of downward flow farther inland on the downwind side of the lake. As a result of reduced surface roughness, there is a reduction in the upward motion near the shoreline (Fig. 10b) and a corresponding reduction in the downward motion over the lake, both mainly restricted to heights below about 1,500 m. Additionally, in a shallow layer where the winds go upslope after reaching the downwind (southern) shore, there are relative upward wind velocities, enhancing the ambient upward motion. These results are also qualitatively

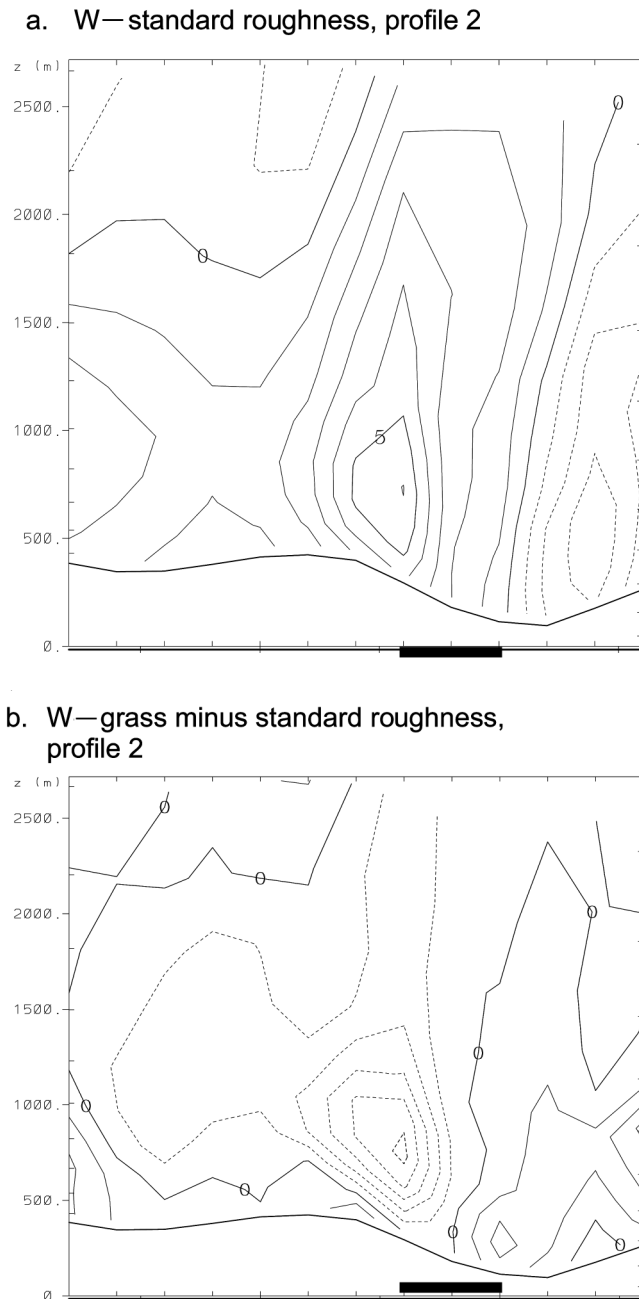


FIG. 10. As in Figure 8, but for profile 2 shown in Figure 7. South is to the left.

similar to those found for the east-west transect shown in Figure 8b.

In an attempt to better understand the increase in precipitation over a band that extends across Lake Ontario, vertical velocities along profile 3 (Fig. 7) are shown in Figure 11. In the standard roughness

case (Fig. 11a), there is general upward motion over Lake Ontario and downward motion to the west of the lake. As stated before, Figure 6 shows evidence of a front near the western end of Lake Ontario, which may be associated with upward motion. The reduction of land surface roughness results in an enhancement of upward motion at low levels over Lake Ontario, except at its western extreme (Fig. 11b). In combination with the high ambient relative humidity (Fig. 6), this should result in an increase and eastward displacement of precipitation, as shown in Figure 3b. However, the reasons for enhanced upward motion over Lake Ontario as well as the local maximum in relative humidity are not entirely clear.

The higher wind speeds over both lake and land, due to lower surface roughness over the land, also affects the lake surface temperature (Fig. 12b). Higher wind speeds allow the absorbed solar radiation to be more readily dissipated by sensible and latent heat fluxes, giving the lake surface a lower temperature. Therefore, the temperatures on Lake Erie are lower in the grass roughness case than in the standard roughness case, with the largest reductions, up to about 0.5°C , occurring next to the southeastern shore, on the lee side relative to the prevailing wind. Assessment of this effect is absent from the literature, because comparison of high and low surface roughness states is not available for observation, and previous modeling studies have not included interactive lake temperatures and sufficiently long time integrations to give evidence of this effect. This reduction in water temperature can reduce the temperature differential between the lake surface and overlying air during the winter, it may not be indicative of a reduction in sensible and latent heat fluxes, which are the means by which the lakes ultimately drive the atmosphere. Therefore, if a drastic change in surface roughness were to occur, some of the rules of thumb for forecasting formation of lake effect precipitation (such as a difference of 13°C between the lake surface and 850 mb level given in Holroyd 1971, or the relevant values of U/L given by Laird *et al.* 2003a, b) may need to be re-examined, to see how both the amount of flux of sensible and latent heat and the static stability of the column help to determine this threshold.

CONCLUDING REMARKS

This paper investigates the sensitivity of lake effect precipitation to changes in land surface rough-

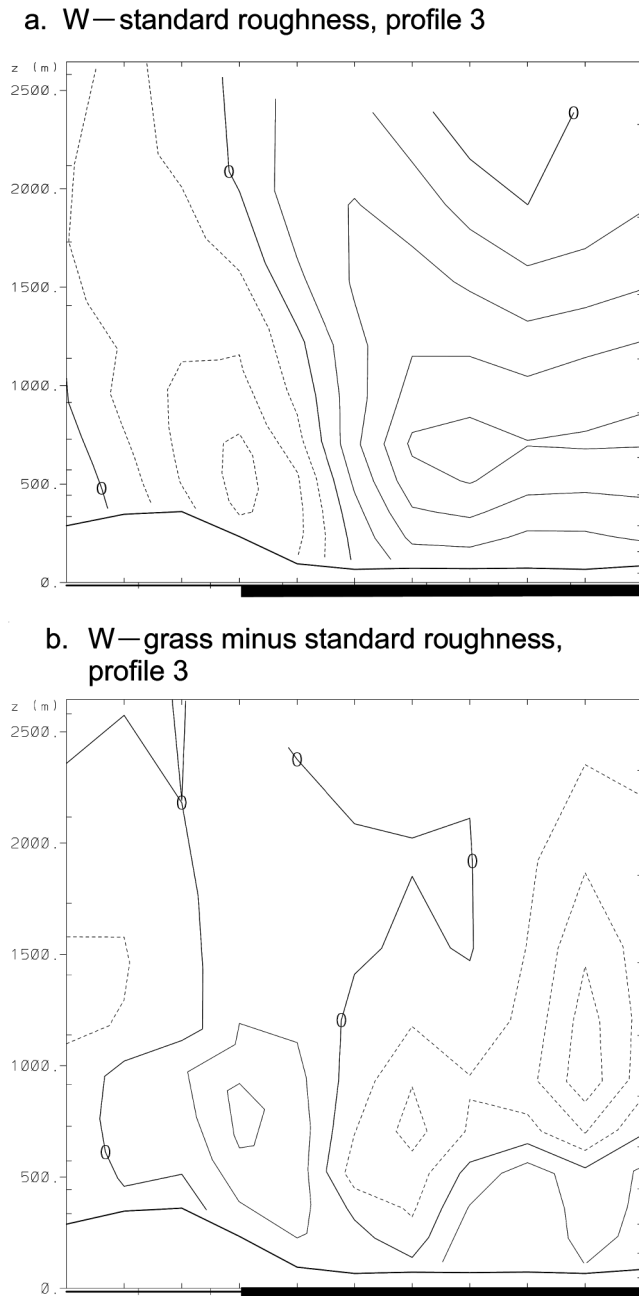


FIG. 11. As in Figure 8, but for profile 3 shown in Figure 7. The dark bars at the bottom of the panels indicate the location of Lake Ontario.

ness applied on a broad spatial scale in the vicinity of the Laurentian Great Lakes, with particular reference to Lake Erie. The grid spacing of the model is 40 km, so results should be regarded as an idealized depiction of the generalized effects of these

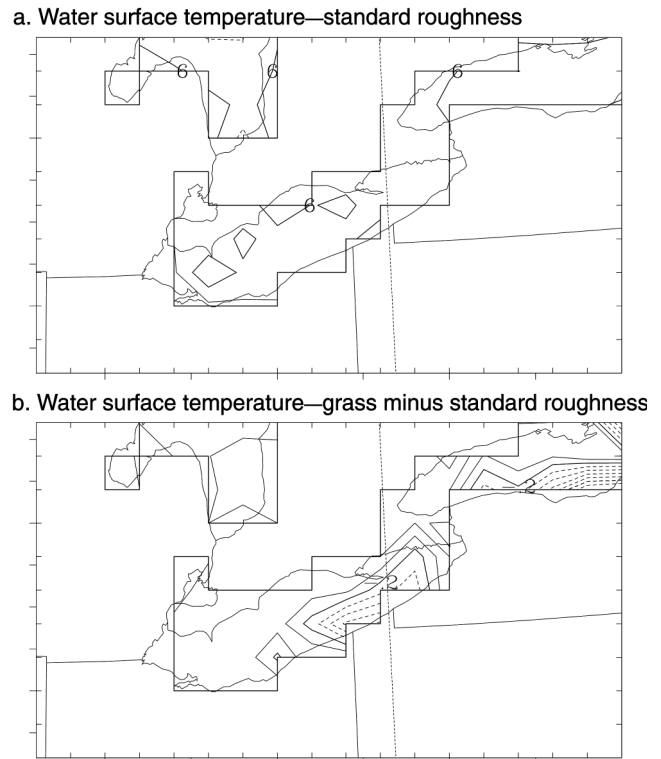


FIG. 12. CHARM 2-simulated lake surface temperature at 06 Z 11 December. (a) The standard roughness case, with a contour interval of 2°C , values of 6°C shown by solid contours, and lesser values shown by dashed contours. (b) The grass roughness case minus the standard roughness case, with a contour interval of 0.1°C , values of -0.2°C or greater shown with solid contours, and lesser values with dashed contours.

changes in roughness, rather than a detailed picture of the constituent snowbands of a lake-effect event.

As expected, a drastic reduction in surface roughness reduces the overall precipitation in the lake effect zone of Lake Erie both on a monthly basis and for a selected event. The reduction on a monthly basis is more concentrated in the area near the lake shore than is the precipitation in the standard roughness case. In the individual case of 11 December 1993, when heavy lake effect precipitation occurred near southeastern Lake Erie, while reduced surface roughness causes reduced precipitation immediately adjacent to the lake, there is a band of increased precipitation farther inland. The forcing of upward motion in many lake effect events is due to rapid, spatially localized deceleration

tion of winds as those winds reach a region of higher surface roughness. The reduction of surface roughness over land and hence its contrast with the lake surface not only reduces the overall amplitude of this upward motion and accompanying precipitation, but also softens its spatial focus, allowing some of the upward motion to occur farther inland. An important part of the reason for enhanced precipitation at locations farther inland appears to be increased speed of upslope winds at low levels in association with topography. Therefore, this result appears to be most relevant where lake effect precipitation occurs in the presence of significant topography, such as near southeastern Lake Erie and southern and eastern Lake Ontario. Nevertheless, in locations such as the eastern shore of Lake Michigan, topography remains important (Hjelmfelt 1992).

In certain parts of the Great Lakes region, including this region near southeastern Lake Erie, there is a particular hydrologic significance to these effects. While lake effect precipitation is usually thought of as carrying water out of the lake but redepositing it within the drainage basin, because the boundary of the drainage basin of Lake Erie is located close to the southeastern shore, a change in the spatial distribution of precipitation would result in more water leaving the Lake Erie drainage basin.

While complete removal of forests in the Great Lakes basin has not occurred (Cole *et al.* 1998), widespread clear-cut logging has occurred during the past slightly more than a century, but forests have recovered some of their extent during more recent times. This paper has captured some of the effects of land use change that occurs at large spatial scale, but much land use change occurs at small scales. One of the most common land transformations occurring at the present time is urbanization. In terms of surface roughness, this often replaces low-roughness cropland with houses and scattered trees, increasing the roughness, although where urban land use replaces a forest, the roughness may decrease. Other land cover parameters will change simultaneously with surface roughness—cropland has different surface albedo, and possibly much greater seasonal variability of albedo, compared to forest and urban land. Leaf area index will also differ; and rooting depth, and hence the potential amount of water storage, will differ, and some fraction of urban land surface will be impermeable to water. Future research may look at the effects of more realistic and comprehensive

reconstructions of land use change during historical times and projections of changes into the future, and numerical prediction at finer granularity. However, this will introduce a tradeoff with regard to available computing power—the more subtle forcing associated with more realistic and localized land use changes will require a larger ensemble of cases to produce significant results, while finer spatial resolution in the model will place greater demands for computing resources.

ACKNOWLEDGMENTS

Thanks to two anonymous reviewers for suggestions to improve this paper. This is GLERL Contribution No. 1405.

REFERENCES

- Cole, K.L., Stearns, F., Guntenspergen, G., Davis, M.B., and Walker, K. 1998. Historical land cover changes in the Great Lakes region. In *Perspectives on the land-use history of North America: a context for understanding our changing environment*. Sisk, T.D., editor. U.S. Geological Survey, Biological Resources Division, Biological Science Report USGS/BRD/BSR 1998-0003 (Revised September 1999).
- Cotton, W.R., and coauthors. 2003. RAMS 2001: Current status and future directions. *Meteor. Atmos. Phys.* 82:5–29.
- Hjelmfelt, M.R. 1990. Numerical study of the influence of environmental conditions on lake-effect snowstorms over Lake Michigan. *Mon. Wea. Rev.* 118:138–150.
- . 1992. Orographic effects in simulated lake-effect snowstorms over Lake Michigan. *Mon. Wea. Rev.* 120:373–377.
- Holroyd, E.W., III. 1971. Lake effect cloud bands as seen from weather satellites. *J. Atmos. Sci.* 28:1165–1170.
- Hostetler, S.W., and Bartlein, P.J. 1990. Simulation of lake evaporation with application to modeling lake level variations of Harney-Malheur Lake, Oregon. *Wat. Resour. Res.* 26:2603–2612.
- Kalnay, E., and coauthors. 1996. The NCEP/NCAR 40-year Reanalysis Project. *Bull. Amer. Meteorol. Soc.* 77:437–471.
- Laird, N.F., and Kristovich, D.A.R. 2004. Comparison of observations with idealized model results for a method to resolve winter lake-effect mesoscale morphology. *Mon. Wea. Rev.* 132:1093–1103.
- , Kristovich, D.A.R., and Walsh, J.E. 2003a. Idealized model simulations examining the mesoscale structure of winter lake-effect circulations. *Mon. Wea. Rev.* 131:206–221.
- , Walsh, J.E., and Kristovich, D.A.R. 2003b.

- Model simulations examining the relationship of lake-effect morphology to lake shape, wind direction, and wind speed. *Mon. Wea. Rev.* 131:2102–2111.
- Liu, A.Q., and Moore, G.W.K. 2004. Lake-effect snowstorms over southern Ontario, Canada, and their associated synoptic-scale environment. *Mon. Wea. Rev.* 132:2595–2609.
- Lofgren, B.M. 2004. A model for simulation of the climate and hydrology of the Great Lakes Basin. *J. Geophys. Res.* 109:D18108, doi:10.1029/2004JD004602.
- Niziol, T.A., Snyder, W.R., and Waldstreicher, J.S. 1995. Winter weather forecasting throughout the eastern United States. Part IV: Lake effect snow. *Weather and Forecasting* 10:61–77.
- Passarelli, R.E., Jr., and Braham, R.R., Jr. 1981. The role of the winter land breeze in the formation of Great Lake snow storms. *Bull. Amer. Meteorol. Soc.* 62:482–491.
- Pielke, R.A., Cotton, W.R., Walko, R.L., Tremback, C.J., Lyons, W.A., Grasso, L.D., Nicholls, M.E., Moran, M.D., Wesley, D.A., Lee, T.J., and Copeland, J.H. 1992. A comprehensive meteorological modeling system—RAMS. *Meteor. Atmos. Phys.* 49:69–91.
- Sousounis, P.J., and Fritsch, J.M. 1994. Lake-aggregate mesoscale disturbances. Part II: A case study of the effects on regional and synoptic-scale weather systems. *Bull. Amer. Meteorol. Soc.* 75:1793–1811.
- , and Mann, G.E. 2000. Lake-aggregate mesoscale disturbances. Part V: Impacts on lake-effect precipitation. *Mon. Wea. Rev.* 128:728–745.
- Walko, R.L., Band, L.E., Baron, J., Kittel, T.G.F., Lambers, R., Lee, T.J., Ojima, D., Pielke, R.A., Sr., Taylor, C., Tague, C., Tremback, C.J., and Vidale, P.J. 2000. Coupled atmosphere-biophysics-hydrology models for environmental modeling. *J. Appl. Meteorol.* 39:931–944.

Submitted: 29 March 2006

Accepted: 19 September 2006

Editorial handling: Barry M. Lesht